JCB Article

In vivo kinetics of Cajal body components

Miroslav Dundr,[1] Michael D. Hebert,[3,4] Tatiana S. Karpova,[2] David Stanek,[5] Hongzi Xu,[3] Karl B. Shpargel,[4] U. Thomas Meier,[6] Karla M. Neugebauer,[5] A. Gregory Matera,[4] and Tom Misteli[1]

[1]National Cancer Institute and [2]Fluorescence Imaging Facility, National Institutes of Health, Bethesda, MD 20892
[3]The University of Mississippi Medical Center, Jackson, MS 39216
[4]Case Western Reserve University School of Medicine, Cleveland, OH 44106
[5]Max Planck Institute of Molecular Cell Biology and Genetics, 01307 Dresden, Germany
[6]Albert Einstein College of Medicine, Bronx, NY 10461

Cajal bodies (CBs) are subnuclear domains implicated in small nuclear ribonucleoprotein (snRNP) biogenesis. In most cell types, CBs coincide with nuclear gems, which contain the survival of motor neurons (SMN) complex, an essential snRNP assembly factor. Here, we analyze the exchange kinetics of multiple components of CBs and gems in living cells using photobleaching microscopy. We demonstrate differences in dissociation kinetics of CB constituents and relate them to their functions. Coilin and SMN complex members exhibit relatively long CB residence times, whereas components of snRNPs, small nucleolar RNPs, and factors shared with the nucleolus have significantly shorter residence times. Comparison of the dissociation kinetics of these shared proteins from either the nucleolus or the CB suggests the existence of compartment-specific retention mechanisms. The dynamic properties of several CB components do not depend on their interaction with coilin because their dissociation kinetics are unaltered in residual nuclear bodies of coilin knockout cells. Photobleaching and fluorescence resonance energy transfer experiments demonstrate that coilin and SMN can interact within CBs, but their interaction is not the major determinant of their residence times. These results suggest that CBs and gems are kinetically independent structures.

Introduction

Cajal bodies (CBs) are evolutionarily conserved nuclear domains present in yeast, animal, and plant cells (Matera, 1999; Gall, 2000; Ogg and Lamond, 2002; Verheggen et al., 2002). This conservation points to important, albeit poorly understood, nuclear functions for these structures. CBs contain a wide variety of components, including factors involved in pre-mRNA splicing, preribosomal RNA (pre-rRNA) processing, and histone pre-mRNA 3′ maturation, as well as basal transcription factors for RNA polymerases I, II, and III and telomerase RNA (Matera, 1999; Gall, 2000; Zhu et al., 2004). Pulse-chase labeling reveals that CBs are not major sites of transcription; the absence of poly A^+ and rRNA within CBs also suggests they are not directly involved in processing these RNAs (Matera, 1999). Many CB components are shared with the nucleolus, and CBs frequently localize to the nucleolar periphery or within nucleoli (Ochs et al., 1994; Gall, 2000; Verheggen et al., 2002). CBs have recently been implicated in post-transcriptional modification of newly assembled spliceosomal U snRNAs (Darzacq et al., 2002; Jady et al., 2003) and in the maturation of small nuclear ribonucleoprotein (snRNP) complexes (Sleeman and Lamond, 1999a; Stanek et al., 2003). Furthermore, they are also likely involved in aspects of snoRNA metabolism, including 5′-cap hypermethylation, 3′-end trimming, and assembly of small nucleolar RNPs (snoRNPs; Carmo-Fonseca, 2002; Verheggen et al., 2002).

CBs are molecularly defined by the presence of the marker protein coilin (Raska et al., 1991). In most cell types and tissues, CBs also contain the survival of motor neurons (SMN) protein (Matera and Frey, 1998; Carvalho et al., 1999; Young et al., 2000). SMN is part of a multiprotein complex that plays an essential role in the assembly of spliceosomal snRNPs (Meister et al., 2002; Paushkin et al., 2002). In the absence of a functional SMN complex, snRNPs are improperly

Address correspondence to M. Dundr, National Cancer Institute, National Institutes of Health, Bethesda, MD 20892. Tel.: (301) 402-0303. Fax: (301) 402-0055. email: dundrm@mail.nih.gov; or A.G. Matera, Case Western Reserve University School of Medicine, Cleveland, OH 44106. Tel.: (216) 368-4922. Fax: (216) 368-1257. email: a.matera@case.edu

Key words: Cajal body; gems; coilin; SMN; iFRAP

Abbreviations used in this paper: CB, Cajal body; iFRAP, inverse fluorescence recovery after photobleaching; FRET, fluorescence resonance energy transfer; MEF, mouse embryonic fibroblast; rRNA, ribosomal RNA; SMN, survival of motor neurons; snRNP, small nuclear ribonucleoprotein; snoRNP, small nucleolar ribonucleoprotein; Tgs1, trimethylguanosine synthase 1.

assembled, resulting in defects in pre-mRNA splicing (Fischer et al., 1997). In some cell lines and certain fetal tissues (Liu and Dreyfuss, 1996; Sleeman and Lamond, 1999b; Young et al., 2001), the SMN complex localizes in separate nuclear structures, called gems (Gemini of CBs). The localization of SMN to CBs is regulated by the methylation status of the RG box in coilin (Boisvert et al., 2002; Hebert et al., 2002).

Using time-lapse fluorescence microscopy in living cells, several groups have shown that CBs are mobile within the nucleoplasm (Boudonck et al., 1999; Platani et al., 2000, 2002). Furthermore, Handwerger et al. (2003) demonstrated that GFP fusions of both coilin and TATA-binding protein are dynamically exchanged between the CB and the nucleoplasm in isolated *Xenopus* oocyte nuclei, although the exchange is slow in comparison to the nucleoplasmic mobility of these proteins (Handwerger et al., 2003). Furthermore, FRAP experiments in mammalian cells suggest rapid exchange of fibrillarin, SMN, and coilin from CBs (Snaar et al., 2000; Sleeman et al., 2003). These observations suggest that CBs are dynamic structures.

In this work, we have systematically investigated the dynamic properties of various CB components. To this end, we have analyzed the kinetics of 14 proteins belonging to several functionally distinct groups of CB components, including factors involved in pre-mRNA splicing, pre-rRNA processing, and snoRNA biogenesis. Using a modified photobleaching technique termed inverse fluorescence recovery after photobleaching (iFRAP), we find three kinetically distinct groups of components within CBs. Furthermore, fluorescence resonance energy transfer (FRET) experiments provide evidence for coilin–SMN, coilin–coilin and SMN–SMN interaction within the CB. The residence times of CB components that localize to residual CBs were not dependent on coilin, and the residence times of coilin and SMN in CBs were independent of their physical interaction. The sum of our observations provides a kinetic framework for CB components in vivo and has implications for the dynamic functional interplay of nuclear subcompartments.

Results

We use iFRAP to study the kinetics of fluorescently tagged CB components in living cells. In iFRAP, the entire nucleus with the exception of a small region of interest containing a CB is bleached using a pulsed laser. The loss of fluorescence signal in the CB is then monitored by time-lapse microscopy. The rate of decay is a good approximation for the dissociation kinetics of the observed protein from the region of interest (Dundr et al., 2002; Phair et al., 2004). iFRAP, as opposed to FRAP, is the method of choice for these experiments because it provides a relatively direct indication of a protein's residence time in a nuclear structure, and the measurement is independent of the size of the structure.

Coilin dynamics

First, we tested the dissociation kinetics of the CB marker protein coilin. To this end, a previously characterized HeLa cell line (Sleeman et al., 1998; Platani et al., 2000) stably expressing GFP-coilin was used (Fig. 1 B). When iFRAP was applied to these cells, a small fraction of the fluorescence signal was lost within the first 5 s after the bleaching event, followed by a slow decline of the CB signal. After ~200 s, a plateau representing the dissociation/association equilibrium of the unbleached population of molecules was reached (Fig. 1 J). Although the rapid initial loss likely reflects of a fraction of loosely bound or diffusing GFP-coilin, the slow loss of the majority of protein indicates that GFP-coilin is temporarily retained in the CB. The ~200-s plateau indicates that coilin resides in mammalian CBs on the order of 2–3 min (Fig. 1 J). Typical measurement errors in all experiments were ~15%. Equivalent results were obtained by transient transfection of full-length GFP-coilin (Fig. 1 A; unpublished data). These results are consistent with the reported dynamic exchange of coilin from CBs in isolated *Xenopus* oocyte nuclei, although *Xenopus* coilin exhibited significantly longer residence times (Handwerger et al., 2003).

To probe in more detail the mechanism of coilin retention in CBs, we transiently expressed a series of previously characterized GFP-coilin deletion mutants (Fig. 1 A; Hebert and Matera, 2000; Hebert et al., 2001; Shpargel et al., 2003). Most of the mutants were generated by progressive truncations of the COOH terminus; the other constructs contained an internal deletion of the RG box or an NH_2-terminal truncation of the self-association domain (Fig. 1, A–I). With the exception of GFP-coilin (94–576), which is entirely nucleoplasmic, all of the mutant constructs localize to CBs when expressed at low to moderate levels (Hebert and Matera, 2000). Notably, the (1–248) and (1–315) constructs show additional accumulations in nucleoli (Fig. 1, D and E). As shown in Fig. 1 J, the iFRAP curves for the (1–248), (1–315), and (1–482) constructs have dissociation kinetics similar to the wild-type protein (Fig. 1 J; $P > 0.1$). In contrast, the (1–92), (1–161), and ΔRG box mutants are distinct from the other constructs during the first 100 s after bleaching ($P < 0.001$ for all). The later portions of all of the curves appear similar to the wild-type protein, suggesting that a common element is responsible for tethering these proteins to CBs. As a control, iFRAP on the (94–576) mutant, which does not localize to CBs, results in very fast loss of signal from a CB-sized region of the nucleoplasm within 5 s (unpublished data). In summary, the domain spanning residues 94–248, which binds to Nopp140 (unpublished data) and contains a cryptic NoLS (Hebert and Matera, 2000) and the RG box, appears to contribute significantly to the CB retention kinetics. Thus, although the primary, steady-state CB localization element is located within the NH_2-terminal domain, two additional regions play important roles in the dynamic retention of coilin in CBs.

Kinetics of splicing and RNP assembly factors

In addition to coilin, the CB contains a large number of components involved in pre-mRNA splicing. To determine the dynamic properties of splicing factors in the CB, we tested the dissociation kinetics of human snRNP core proteins GFP-SmB (Fig. 2 A), GFP-SmD1 (Fig. 2 B), and the U4/U6 snRNP assembly factor GFP-SART3 (Fig. 2 C) in transiently transfected HeLa cells. GFP-tagged versions of these proteins have previously been demonstrated to be incorporated into snRNPs or to interact with them (Sleeman

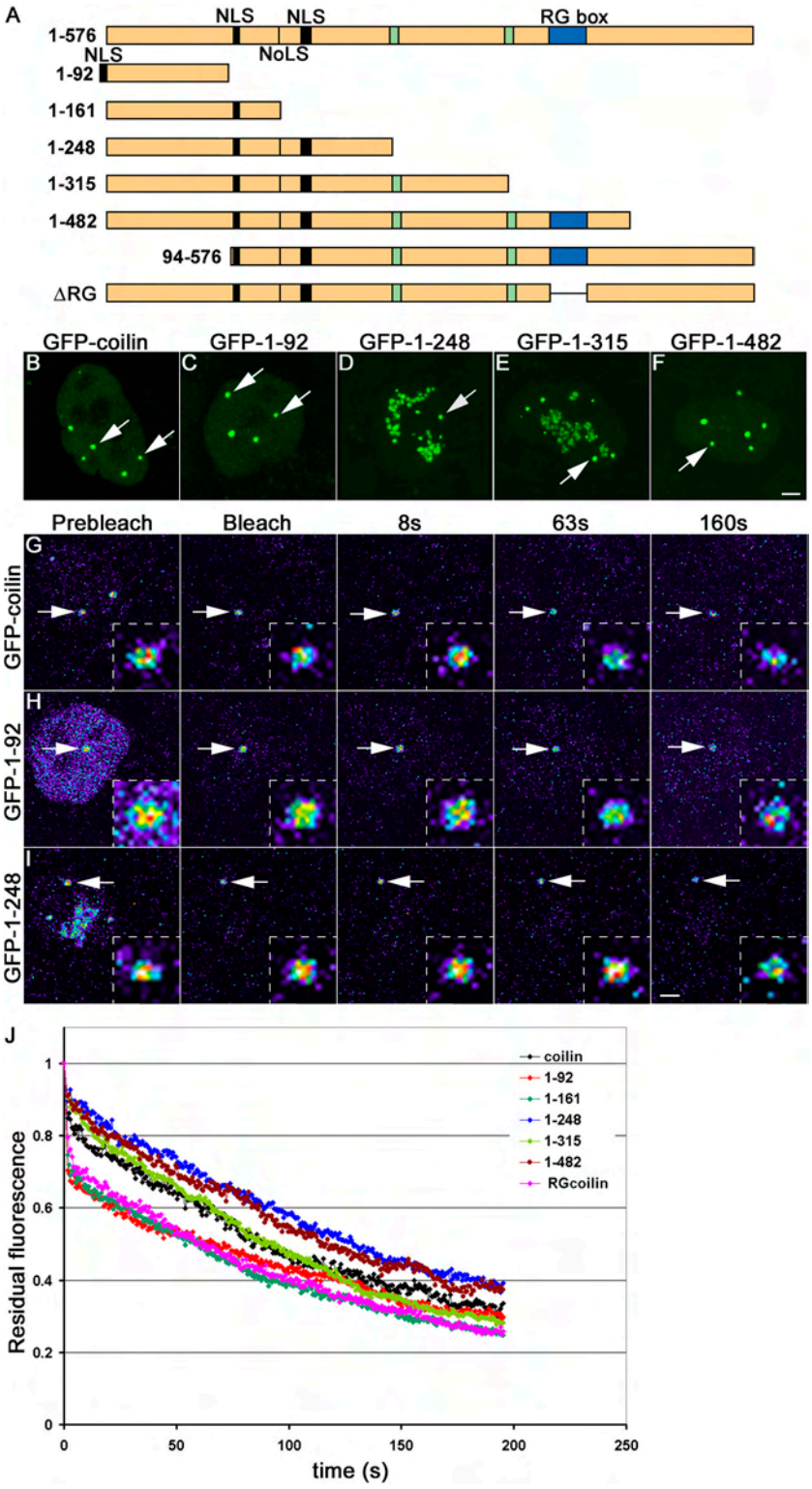

Figure 1. **iFRAP on coilin and coilin mutants.** (A) Full-length coilin (1–576) and coilin mutants fused to GFP at the NH_2 terminus. The putative coilin nucleolar localization signal (NoLS), nuclear localization signals (NLS), and serine patches from amino acids 242–259 and 312–325 (green boxes) are indicated. The NLS in the mutant (1–92) was added exogeneously. (B–F) Localization of GFP-coilin (B), GFP-coilin 1–92 (C), GFP-coilin 1–248 (D), GFP-coilin 1–315 (E), and GFP-coilin 1–482 (F) in HeLa cells. CBs are indicated by arrows. Note that mutants 1–248 and 1–315 are also present in nucleoli. (G–I) iFRAP on GFP-coilin (G), GFP-coilin 1–92 (H), and GFP-coilin 1–248 (I). Cells were imaged before and after photobleaching of the entire nucleus with the exception of one CB. The loss of fluorescent signal was monitored using time-lapse microscopy. The unbleached CBs monitored are indicated by arrows and are shown as enlarged insets. Pseudocolored images are shown with high signal levels in red/yellow and low signals in blue. (J) Quantification of iFRAP kinetics. Mutants 1–92, 1–161, and ΔRG showed faster loss than wild-type and the other mutants. Averages from at least 20 cells from two independent experiments are shown. Typical measurement errors were ~15%. Bars, 2 μm; insets, 0.5 μm.

and Lamond, 1999a; Stanek et al., 2003; unpublished data), suggesting that these proteins are functional. Consistent with their presence in a discrete complex, the fluorescence decay curves for the Sm proteins were superimposable, and these proteins displayed dissociation kinetics that were significantly faster than GFP-coilin (Fig. 2 D; $P < 0.001$). More than 50% of the initial fluorescence signal was lost within 30 s, whereas in comparison, 50% reduction for GFP-coilin was only reached after 100 s (Fig. 2 D). The U4/U6 snRNP assembly factor SART3 showed even more rapid dissociation from CBs (Fig. 2 D; $P < 0.001$), consistent with biochemical data suggesting a transient association of SART3 with the U4/U6 snRNP (Bell et al., 2002; Stanek et al., 2003). Together, these observations suggest that pre-mRNA splicing factors have significantly shorter residence times in CBs than coilin.

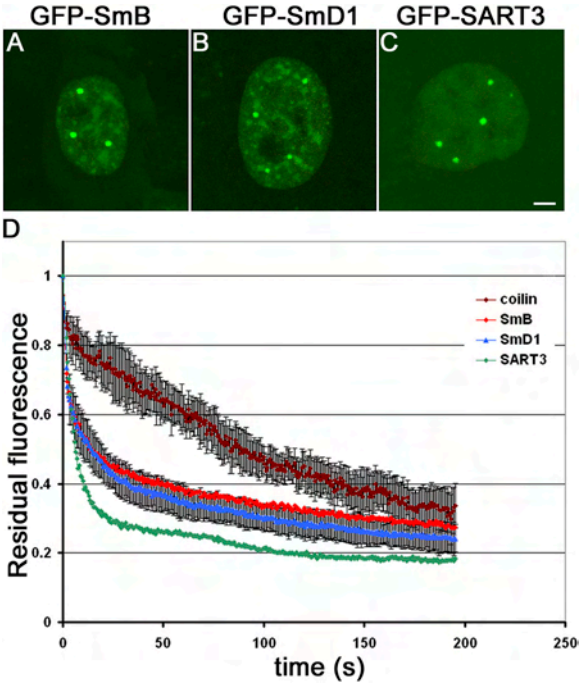

Figure 2. **iFRAP of spliceosomal CB components.** (A–C) Localization of spliceosomal CB components GFP-SmB (A), GFP-SmD1 (B), and GFP-SART3 (C). (D) Quantification of iFRAP kinetics. GFP-SmB and GFP-SmD1 exhibit similar dissociation kinetics from CBs, which are faster than GFP-coilin loss. In contrast, GFP-SART3 is only transiently associated with CBs. Values represent averages from at least 20 cells ± SDs. Bar, 2 μm.

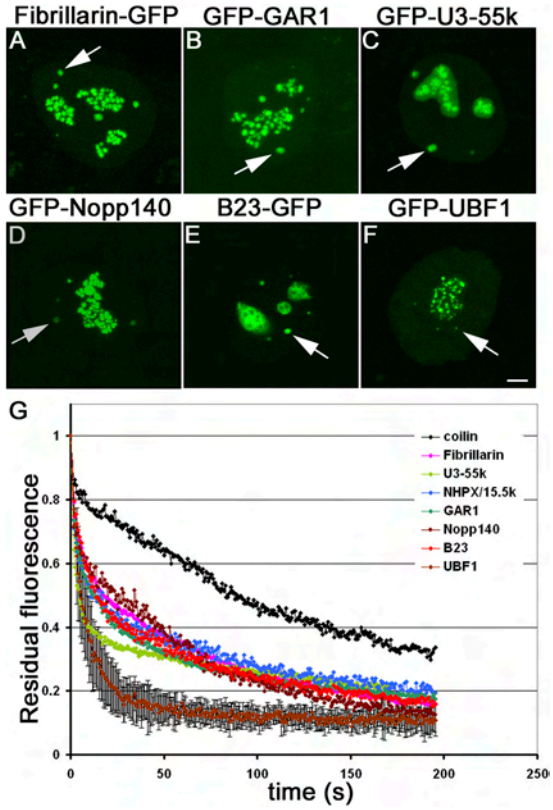

Figure 3. **iFRAP of nucleolar CB components.** (A–F) Localization of nucleolar CB components in HeLa cells. (A) fibrillarin-GFP, (B) GFP-GAR1, (C) GFP-U3–55k, (D) GFP-Nopp140, (E) B23-GFP, and (F) GFP-UBF1. (G) Quantification of iFRAP kinetics. All nucleolar CB components followed similar dissociation kinetics from CBs with the exception of GFP-UBF1. GFP-coilin dissociation kinetics are show for comparison. Values represent averages from at least 20 cells ± SDs. Bar, 2 μm.

The observation that U3 snoRNA precursors accumulate in CBs has led to the proposal that the CB represents a site of snoRNP assembly before transport to their sites of action in the nucleolus (Verheggen et al., 2002). Accordingly, several snoRNP-processing factors localize both to the nucleolus and the CB. To analyze the dissociation kinetics of CB components involved in the assembly and the maturation of U3 snoRNP, we performed iFRAP on two protein components of U3 snoRNP. NHPX/15.5k associates with 3′-extended, monomethylated U3 precursors and also U4/U6 snRNP, whereas fibrillarin associates with the mature U3 snoRNP (Verheggen et al., 2002). In iFRAP analyses, GFP-NHPX and fibrillarin-GFP showed dissociation kinetics similar to the other snoRNP components, consistent with the possibility that they are in the same complex (Fig. 3 G; $P > 0.1$). Additionally, we also tested the dissociation kinetics of CB proteins involved in pseudouridylation, ribose methylation, processing, and transcription of pre-rRNAs: GFP-GAR1 (Fig. 3 B), GFP-Nopp140 (Fig. 3 D), B23-GFP (Fig. 3 E), and GFP-UBF1 (Fig. 3 F). GFP-U3-55k (Fig. 3 C) showed virtually identical dissociation kinetics, but did exhibit a somewhat faster initial loss of signal (Fig. 3 G). The iFRAP data demonstrate that these components dissociated more rapidly from the CB than coilin ($P < 0.001$), but with kinetics similar to the spliceosomal core proteins (Fig. 2 D; $P > 0.1$). More than 50% of the initial fluorescence signal was lost within 30 s, whereas in comparison, 50% reduction for GFP-coilin was only reached after 100 s (Fig. 3 G). Thus, factors involved in modification and processing of pre-rRNA including fibrillarin-GFP, GFP-NHPX/15.5k, GFP-GAR1, GFP-Nopp140, B23-GFP, and possibly GFP-U3-55k share similar dissociation kinetics. In contrast, the RNA polymerase I transcription factor GFP-UBF1 exhibited significantly faster dissociation kinetics from CBs. More than 50% of the initial fluorescence signal in the CB was lost within 5 s, suggesting only very transient association with CBs.

Compartment-specific retention of nucleolar components in CBs

To evaluate whether components that are shared between the CB and the nucleolus are retained in the two compartments by the same or different retention mechanisms, we performed iFRAP on several of these shared components in either nucleoli or CBs. Fibrillarin-GFP, GFP-Nopp140, and B23-GFP exhibited similar dissociation kinetics from CBs ($P > 0.1$). The dissociation kinetics of all proteins from nucleoli were significantly slower, and >50% of the initial fluorescence signal of fibrillarin-GFP and GFP-Nopp140 was lost within 120 s and B23-GFP within 200 s, whereas the same fraction of fluorescence signal was lost within 30 s in CBs (Fig. 4; $P < 0.001$). The differences in loss kinetics are not due to the different sizes of the two compartments

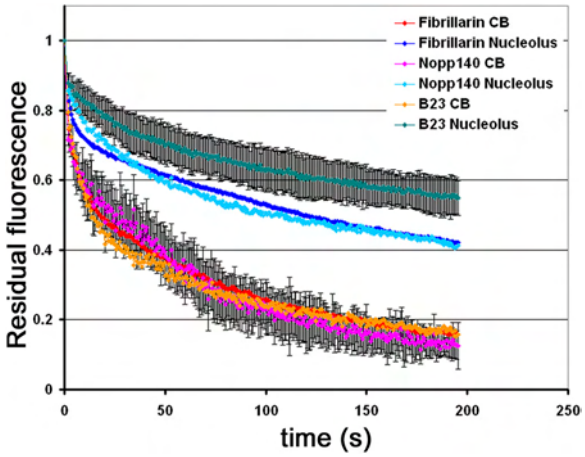

Figure 4. **Compartment-specific retention mechanism in CBs and nucleoli.** Quantification of iFRAP kinetics. The nucleolar CB components, fibrillarin-GFP, GFP-Nopp140, and B23-GFP exhibit significantly faster dissociation kinetics from CBs compared with nucleoli, indicating that they are retained in both nuclear compartments by specific retention mechanisms. Values represent averages from at least 20 cells ± SDs.

because partial bleaching of the nucleolus yields identical results. In addition, the mutant coilin 1–248, which resides both in the CB and the nucleolus, showed identical dissociation kinetics in the two compartments (unpublished data). Together, the observed differences suggest the existence of compartment-specific retention mechanisms for proteins in CBs and nucleoli.

Coilin is not required for retention

Because coilin is the most prominent CB marker and has been suggested to be a structural component of CBs, it might play a critical role in the retention of other CB components within this nuclear suborganelle (Hebert and Matera, 2000). To address this question, we made use of mouse embryonic fibroblasts (MEFs) derived from coilin knockout mice containing residual nuclear bodies enriched in nucleolar components (Tucker et al., 2001; Jady et al., 2003). The dissociation kinetics of GFP-Nopp140, fibrillarin-GFP, and GFP-GAR1 from residual CBs in coilin$^{-/-}$ cells are similar to those in control cells ($P > 0.1$), indicating that coilin is not required for determining the residence of these nucleolar proteins in CBs (Fig. 5). Dissociation kinetics of fibrillarin-GFP and GFP-GAR1 were somewhat faster in MEF cells than in HeLa cells. The t_{50} for both proteins in MEFs were ~10 s, whereas they were ~20 s in HeLa cells. In contrast, no significant difference was observed for GFP-Nopp140 (compare Fig. 3 with Fig. 5).

SMN and coilin have similar residence times in the CB

In most cell types, CBs and gems overlap completely (Liu and Dreyfuss, 1996; Matera and Frey, 1998; Carvalho et al., 1999; Sleeman and Lamond, 1999b). The interaction of coilin and SMN requires symmetrically dimethylated arginines in the coilin RG box (Hebert et al., 2002). To compare the dissociation kinetics of coilin and SMN from CBs, we performed iFRAP on GFP-SMN (Fig. 6 A), which was

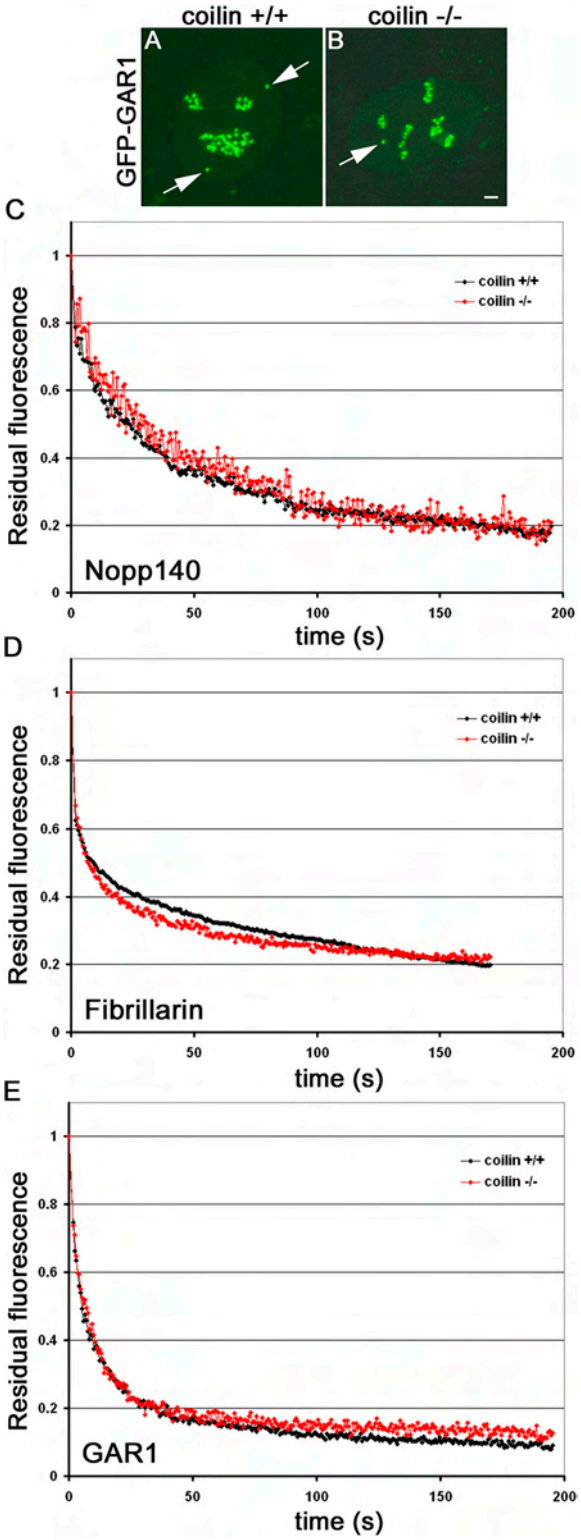

Figure 5. **Coilin-independent dissociation kinetics.** (A and B) GFP-GAR1 was expressed in coilin$^{+/+}$ MEFs (A) or in coilin$^{-/-}$ MEFs (B). In contrast to the normal localization of GFP-GAR1 in coilin$^{+/+}$ cells (A, arrow), in the absence of coilin GFP-GAR1 localized in residual CBs (B, arrow). (C–E) Quantification of iFRAP kinetics. The dissociation kinetics of GFP-Nopp140 (C), which directly interacts with coilin, fibrillarin-GFP (D), and GFP-GAR1 (E) from CBs is unaffected in the absence of coilin. Averages from at least 20 cells are shown. Typical measurement errors were ~15%. Bar, 2 μm.

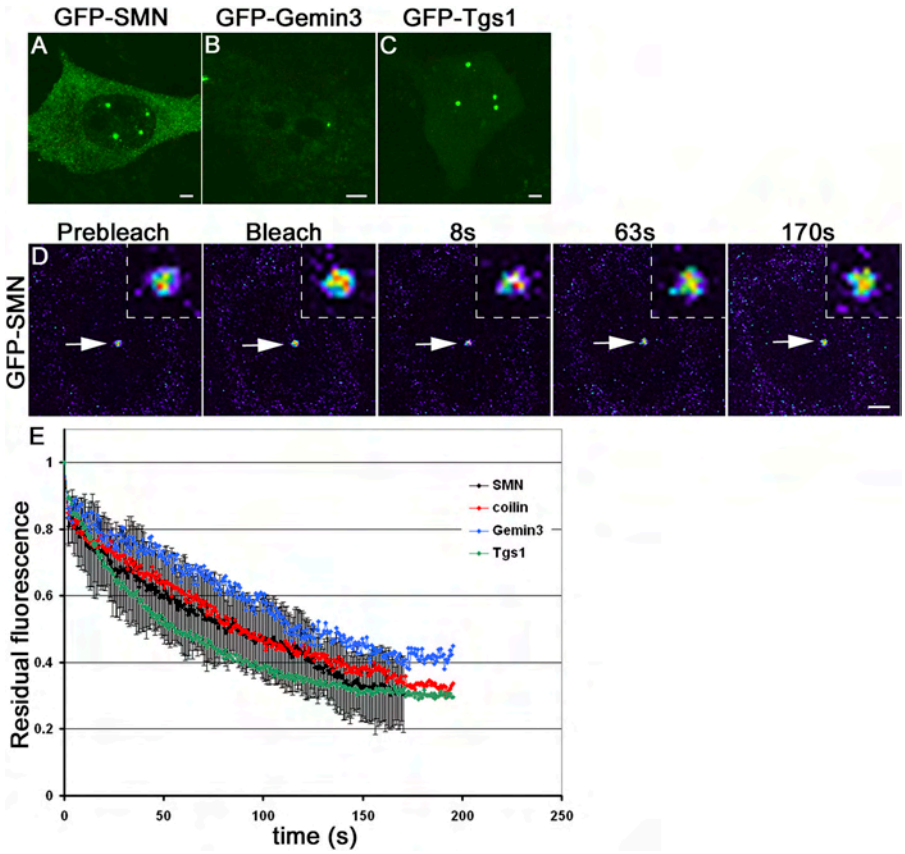

Figure 6. **iFRAP on RNP assembly machinery.** (A–C) Localization of expressed gem components in HeLa cells. (A) GFP-SMN, (B) Gemin3-GFP, and (C) GFP-Tgs1. (D) Cells expressing GFP-SMN were imaged before and after photobleaching of the entire nucleus with the exception of one CB/gem as shown in pseudocolor. The unbleached CB/gem monitored is indicated by arrows and is shown as enlarged insets. (E) Quantification of iFRAP kinetics. The components of SMN protein complex, GFP-SMN, Gemin3-GFP, and GFP-Tgs1 exhibit similar dissociation kinetics from CBs. Values represent averages from at least 20 cells ± SDs. Bars, 2 μm; insets, 0.5 μm.

previously characterized and shown to coimmunoprecipitate with Gemin2 (Sleeman et al., 2003), a core member of the SMN complex. The loss of GFP-SMN fluorescence in CBs was nearly identical to that of GFP-coilin, indicating that both proteins have similar CB residence times (Fig. 6 E), consistent with biochemical data demonstrating their physical interaction (Hebert et al., 2001).

To further explore the kinetic behavior of the SMN protein complex in CBs, the dissociation kinetics of another core member of the SMN protein complex, Gemin3, was measured (Fig. 6 B). Gemin3-GFP had similar dissociation kinetics as both SMN and coilin (Fig. 6 E). Furthermore, the dissociation kinetics of GFP-Tgs1 (Fig. 6 C), the trimethylguanosine synthase, were similar to those of GFP-SMN and Gemin3-GFP (Fig. 6 E; $P > 0.05$). Because hTgs1 was recently shown to directly interact with SMN (Mouaikel et al., 2003), these observations indicate that certain SMN-interacting partners reside in CBs for longer periods of time than do snRNP and snoRNP components.

Coilin and SMN interact in the CB in vivo

Because coilin and SMN have similar CB retention dynamics (Fig. 6), we were interested to test whether coilin physically interacts with SMN within the CBs of intact living nuclei. Previous work has shown that SMN and coilin form complexes in vivo (Hebert et al., 2001), and that methylation of the coilin RG box motif is required for recruitment of SMN to CBs (Hebert et al., 2002). However, it was not clear from the biochemical data whether SMN and coilin interact in the nucleoplasm, the CB, or in both places. To test whether these proteins interact in CBs, we performed FRET by acceptor photobleaching in living cells (Karpova et al., 2003; see Materials and methods for details). In acceptor photobleaching FRET, energy transfer between the donor and the acceptor is reduced or eliminated when the acceptor is irreversibly bleached, resulting in an increase in donor fluorescence as an indicator of physical interaction between the test proteins (Karpova et al., 2003). CFP-coilin and YFP-SMN were coexpressed in HeLa cells, the YFP-SMN acceptor was bleached, and the fluorescent signal of CFP-coilin was monitored in living cells (Fig. 7 A). Upon bleaching, an ~6.5 ± 1.2% increase in donor CFP-coilin fluorescence was observed, indicating an in vivo interaction of coilin and SMN in CBs (Fig. 7 B). Reversal of the tags to CFP-SMN and YFP-coilin gave a similar increase in donor CFP-SMN fluorescence of ~6.29 ± 1.3% (unpublished data). A fusion protein between CFP and YFP served as a positive control and yielded a 14 ± 1.3% increase in fluorescence signal (Fig. 7 B). As negative controls, an increase of <0.5 ± 0.2% was observed for coexpressed CFP and YFP, and a loss of fluorescence signal was detected in a CB in the same nucleus to which no acceptor bleaching had been applied (Fig. 7 B). To demonstrate that the positive FRET signal was not merely due to the accumulation of the two proteins in the CB, we performed FRET between fibrillarin-CFP and YFP-coilin or fibrillarin-CFP and YFP-SART3, which are all concentrated in the CB but have not been found to physically interact. FRET signals for these pairs were similar to negative controls and were 0.75 ± 0.54 for fibrillarin/SART3 and 1.19 ± 0.61 for fibrillarin/coilin (Fig. 7, E and F). Interaction of coilin and SMN in the nucleoplasm could not be accurately assessed due to the low nucleoplasmic signal of

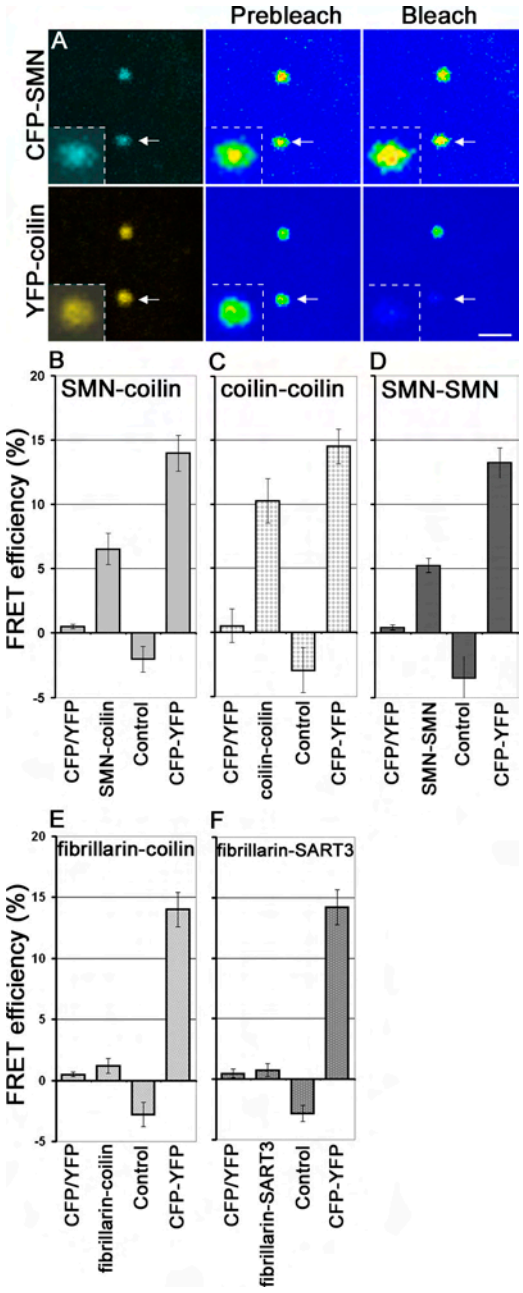

Figure 7. **Coilin and SMN interact in CBs in vivo.** Acceptor bleaching FRET was performed on living HeLa cells coexpressing (A) CFP-SMN and YFP-coilin. The acceptor (YFP-coilin) was irreversibly bleached, resulting in an increase in donor (CFP-SMN) fluorescence, suggestive of physical interaction between coilin and SMN. Note the increase of fluorescence intensity of CFP-SMN in pseudocolored CB after the bleach (arrow, inset). (B–F) Quantification of FRET. A fusion protein between CFP and YFP was used as a positive control. Coexpressed monomeric CFP and YFP and a CB in the same nucleus to which no acceptor bleaching had been applied were used as negative controls. A significant increase of CB donor fluorescence in CBs was detected for CFP- SMN/YFP-coilin (B), CFP-coilin/YFP-coilin (C), CFP-SMN/YFP-SMN self-interaction (D), fibrillarin-CFP/YFP-coilin (E), and fibrillarin-CFP/YFP-SART3 (F). Averages from at least 20 cells are shown. Error bars represent SEM. Bar, 2 μm.

SMN (unpublished data). Furthermore, when purified, recombinant proteins are incubated in vitro, coilin and SMN each have the ability to self-oligomerize (Lorson et al., 1998; Hebert and Matera, 2000). To test whether these proteins self-interact in vivo in CBs, we performed acceptor FRET between CFP-coilin and YFP-coilin or CFP-SMN and YFP-SMN (Fig. 7, C and D). An ~10.26 ± 1.7% increase of CB donor fluorescence was detected for CFP-coilin, and an ~5.23 ± 0.6% increase of CB donor fluorescence was detected for CFP-SMN (Fig. 7, C and D). We conclude that coilin interacts with SMN and that both proteins self-interact in the CB in vivo.

CBs and gems are kinetically independent structures

Our observation that coilin and SMN interact with each other in vivo and have similar CB residence times led us to investigate whether the residence times of the two proteins depends on their mutual presence. To test this possibility, we coexpressed CFP-coilin and YFP-SMN in HeLa cells in the presence of an untagged version of the coilinΔRG mutant. This mutant construct is defective in its interaction with SMN, but retains the ability to localize in CBs (Hebert et al., 2001). Thus, in a wild-type coilin background (i.e., in HeLa cells), overexpression of untagged coilinΔRG should result in formation of distinct YFP-SMN foci (i.e., gems). As expected, in the absence of untagged coilinΔRG, CFP-coilin and YFP-SMN colocalized in CBs and gems were not observed (Fig. 8 A). However, in the presence of an excess of coilinΔRG, YFP-SMN protein was mislocalized in gems (Fig. 8 B). A fraction of the YFP-SMN signal colocalized with CFP-coilin in CBs, presumably due to the presence of endogenous coilin (Fig. 8 B). However, in a large number of cases, overexpression of coilinΔRG resulted in the physical separation of CBs, and no distinct gems (Fig. 8 B). The induced separation allowed us to independently assess the kinetics of the tagged coilin and SMN proteins in CBs and gems. iFRAP analysis revealed that coilin and SMN display the same dissociation kinetics from their separated nuclear bodies as they do in combined CB/gem cells (Fig. 8, C and D; $P > 0.1$). To confirm the similar dissociation kinetics of coilin and SMN from separated CBs and gems, respectively, we performed iFRAP on HeLa-PV cells in which CBs and gems are naturally separated (Liu and Dreyfuss, 1996). Confirming our observations, we find virtually identical iFRAP kinetics for coilin from combined CBs in wild-type cells and separated CBs in HeLa-PV cells (Fig. 8 E; $P > 0.1$). Similarly, we find identical iFRAP kinetics for SMN from combined gems in wild-type cells and separated gems in HeLa-PV cells (Fig. 8 F; $P > 0.1$). Furthermore, for SMN these results were confirmed in coilin knockout cells (Fig. 8 G), where gems are distinct from residual CBs (Tucker et al., 2001). In these cells, YFP-SMN had dissociation kinetics similar to those in control wild-type cells and in gems separated from CBs by overexpression of coilinΔRG (Fig. 8 G; $P > 0.1$). These results demonstrate that the kinetic properties of coilin and SMN are independent of the integrity of the combined CB/gem structure.

Self-interaction of coilin and SMN in separated CBs and gems

The simplest explanation for the observed kinetic independence of CBs and gems is that coilin and SMN residence times are determined by their respective homotypic interac-

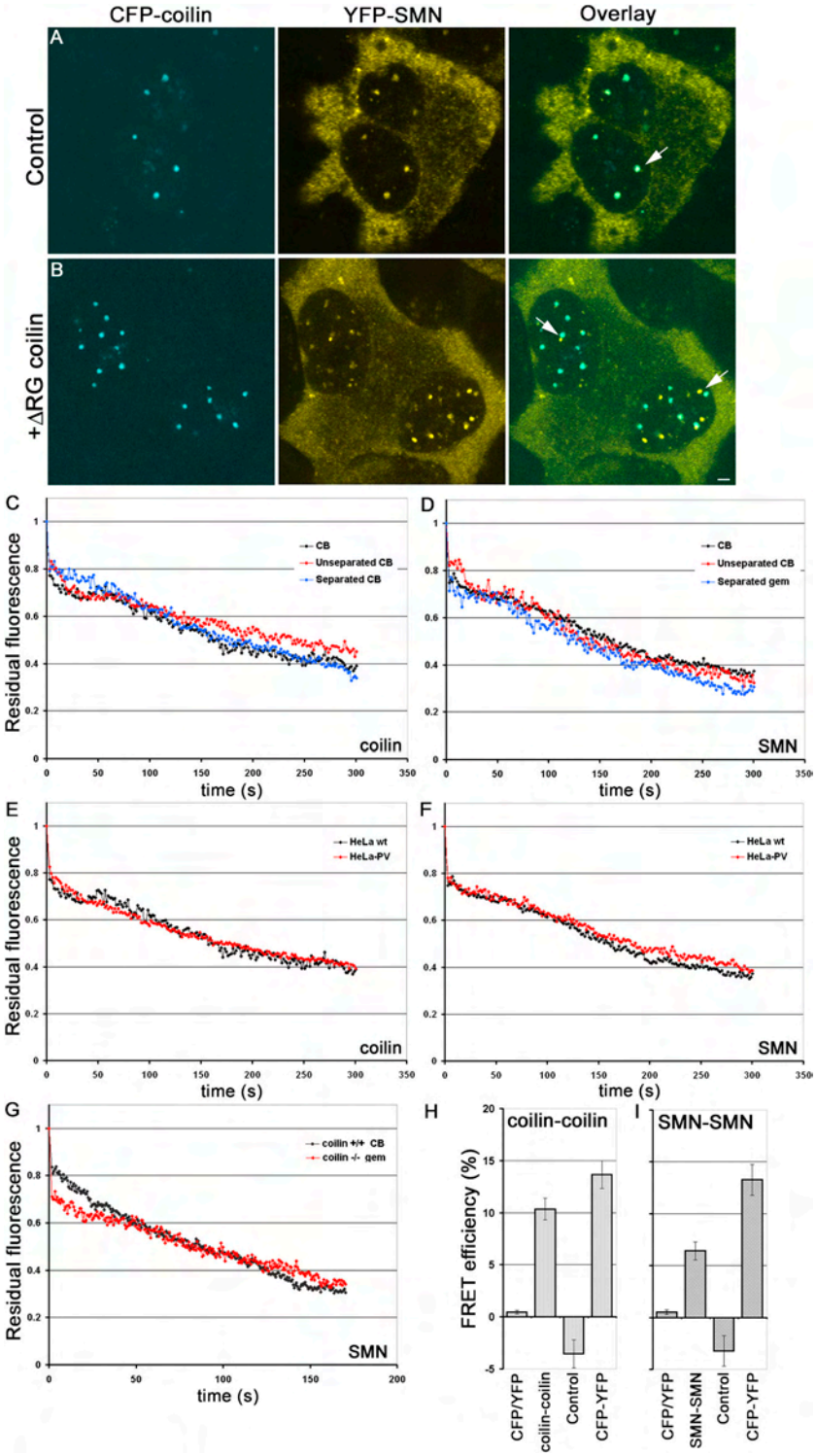

Figure 8. **CB and gems are kinetically independent domains.** (A) CFP-coilin and YFP-SMN colocalize in CBs in HeLa cells (arrow). (B) When CFP-coilin and YFP-SMN are coexpressed with an untagged dominant ΔRG coilin mutant, CBs physically separate from gems (arrows). (C–G) Quantification of iFRAP kinetics. (C and D) YFP-coilin and YFP-SMN exhibit indistinguishable dissociation kinetics in their respective separated organelles as in unseparated CB/gems in control cells. (E and F) YFP-coilin and YFP-SMN exhibited indistinguishable dissociation kinetics from CBs and gems, respectively, in HeLa wild-type and HeLa-PV cells where CBs and gems are naturally separated. (G) GFP-SMN also shows similar dissociation kinetics in coilin$^{-/-}$ cells where gems are naturally separated from residual CBs. Averages from at least 20 cells are shown. (H and I) Self-interaction of coilin and SMN in separated CBs and gems detected by FRET in living cells. Acceptor bleaching FRET was performed on CFP and YFP pairs of coilin or SMN coexpressed with untagged ΔRG coilin mutant. Upon bleaching of separated CBs or gems, significant increases in donor fluorescence of CFP-coilin (H) and CFP-SMN (I) were observed, indicating that both coilin in CBs and SMN in gems self-interact even when CBs and gems are physically separated. Averages from at least 20 cells are shown. Typical measurement errors in iFRAP experiments were ∼15%. Bar, 2 μm.

tions. A prediction from this model is that coilin and SMN maintain self-interactions within separated CBs and gems. To directly test this prediction, pairs of CFP- and YFP-tagged coilin or SMN were expressed together with the untagged coilinΔRG mutant. The self-interaction potential of coilin and SMN in the separated CBs and gems was then tested by FRET in living cells. Upon bleaching, we observed an ∼10.3 ± 1% increase in donor CFP-coilin fluorescence and an ∼6.4 ± 0.9% increase in donor CFP-SMN fluorescence (Fig. 8, H and I). These experiments show that homotypic coilin–coilin and SMN–SMN interactions are maintained in physically separated CBs and gems.

Discussion

We have analyzed the dynamic properties of a number of protein components of CBs in intact, living cells using photobleaching microscopy. We identify three distinct kinetic

groups of CB components, and provide evidence that coilin alone does not determine the dissociation kinetics of CBs. Most importantly, our results suggest that the kinetic properties of CB/gem components are independent of the physical association of the two compartments.

Kinetically distinct CB components

In comparing the dissociation kinetics of 14 CB proteins using iFRAP, we found three distinct kinetic classes. The group of CB proteins with the longest residence times includes coilin, SMN, Gemin3, and Tgs1. These proteins typically reside in CBs on the order of minutes. Consistent with previous biochemical and subcellular localization analyses (Carvalho et al., 1999; Hebert et al., 2001, 2002), we provide direct evidence for an interaction of SMN and coilin within CBs by FRET analysis. We cannot directly determine whether these complexes are stable within the nucleoplasm or if they exchange from CBs as intact complexes. However, the comparable retention dynamics of SMN-associated proteins are consistent with this latter possibility. Thus, the SMN complex might not only exist during early steps of Sm assembly in the cytoplasm, but might also remain associated with the assembled snRNPs after their import into the nucleus, perhaps functioning in later steps of snRNP maturation in CBs (Narayanan et al., 2002; Jady et al., 2003; Sleeman et al., 2003). This interpretation is consistent with heterokaryon assays showing that newly imported GFP-Sm proteins are targeted only into CBs that contain SMN (Sleeman et al., 2001). This scenario is also supported by our observation of similar dissociation kinetics of GFP-Tgs1 and GFP-SMN and by the recent finding that Tgs1 physically associates with the SMN complex (Mouaikel et al., 2003). Furthermore, the observation that 3′-extended U3 snoRNA precursors with a monomethylated m^7G-cap were detected in CBs also suggests that 5′-cap trimethylation of U3 snoRNA occurs in CBs (Verheggen et al., 2002).

The second kinetic group of CB proteins contains nucleolar snoRNP components and the spliceosomal snRNP core proteins. These proteins have significantly faster dissociation kinetics than coilin and the SMN-associated proteins. We find that fibrillarin-GFP, a box C/D snoRNP factor, and the box H/ACA snoRNP component GAR1 have similar dissociation kinetics from CBs, suggesting that the two snoRNP classes might have analogous mechanisms of retention in CBs. This latter scenario is supported by the fact that GFP-Nopp140, which is associated with both classes of snoRNPs, exhibited comparable dissociation kinetics from CBs as both snoRNP classes. Because 3′-extended precursor U3 snoRNA is only associated with NHPX/15.5k but not with fibrillarin, our data are consistent with findings that the majority of U3 snoRNA detected in CBs are mature U3 snoRNPs (Verheggen et al., 2002). The dissociation kinetics of these proteins was significantly slower than that of the third (and fastest) kinetic group containing the U4/U6 assembly factor SART3 (Bell et al., 2002) and RNA polymerase I transcription factor UBF1. GFP-SART3 exhibited dissociation kinetics, indicating that its association with CBs lasts only a few seconds. This kinetic behavior is in agreement with the observation that SART3 is only transiently associated with snRNPs, and supports a model in which SART3 delivers U6 to the CB where U4/U6 snRNP (re)assembly may occur (Bell et al., 2002; Stanek et al., 2003).

The rapid exchange dynamics of CB components, in the range of seconds to minutes, indicates that all measured proteins are dynamic and are continuously exchanged between the nucleoplasm and CBs. Proteins are likely retained in CBs via transient interaction with less mobile CB components. The dynamic nature of CB association also suggests that any putative modification steps taking place within the CB are relatively rapid and occur on the order of seconds. Furthermore, our observations are consistent with the possibility that many proteins may enter CBs nondiscriminatorily and that collisions with interacting partners lead to their retention. This scenario might explain why certain CB components are retained in CBs only when their partner protein is present, for example in a cell cycle–dependent manner such as cyclin E and $p220^{NPAT}$, a substrate of the CB component cyclin E/cdk2 (Liu et al., 2000; Wei et al., 2003).

The observed dynamic nature of CB components is in agreement with the demonstration of dynamic exchange of proteins from several other nuclear compartments, including nucleoli and splicing factor compartments (Phair and Misteli, 2000; Snaar et al., 2000; Chen and Huang, 2001; Dundr et al., 2002; Handwerger et al., 2003; Sleeman et al., 2003). In contrast, at least some components of promyelocytic leukemia bodies appear to be more stably associated (Boisvert et al., 2001). Dynamic exchange of CB components has also been demonstrated for coilin, TATA-binding protein, and U7 snRNA from CBs in *Xenopus* germinal vesicles, although in this system coilin resides in CBs for up to ~30 min (Handwerger et al., 2003). The reason for the significantly longer residence time of coilin in CBs from *Xenopus* is unclear, but might be due to lower levels of rRNA and snRNA metabolism. In agreement with our observations, a rapid exchange of fibrillarin and coilin from CBs in mammalian cells has previously been reported (Snaar et al., 2000; Sleeman et al., 2003). In contrast to our iFRAP experiments, FRAP analysis has suggested slower exchange of SMN compared with coilin (Sleeman et al., 2003). The apparent discrepancy is likely explained by different measurement technique and the smaller nucleoplasmic pool of SMN compared with coilin (Sleeman et al., 2003). Because FRAP recovery kinetics (but not iFRAP loss kinetics) are sensitive to the size of the unbleached pool, the smaller unbleached nucleoplasmic pool of GFP-SMN compared with GFP-coilin may result in underestimation of exchange kinetics when using FRAP.

Compartment-specific retention mechanisms

Comparison of the dissociation kinetics of nucleolar components that also localize in CBs revealed that nucleolar CB components reside in CBs for a significantly shorter time than they do in nucleoli, indicating the existence of compartment-specific retention mechanisms. These kinetic differences between CBs and nucleoli might be due to interactions of the nucleolar pool of the processing components with pre-rRNA during modification and maturation steps. Because CBs do not contain any pre-rRNA transcripts, retention is reduced in CBs, resulting in faster dissociation. This interpretation is supported by the fact that truncated

mutants of fibrillarin-GFP lacking the RNA-binding domain exhibit significantly faster kinetics in nucleoli than wild-type fibrillarin (Snaar et al., 2000). Similarly, when nucleolar rRNA transcription is selectively inhibited by actinomycin D, pre-rRNA processing components nucleolin, fibrillarin, B23, and Rpp29 exhibit faster kinetics in the nucleoli (Chen and Huang, 2001). In contrast, the inhibition of transcription of all three RNA polymerases by actinomycin D does not affect the dissociation kinetics of coilin from CBs, although the structures are relocated to the nucleolar periphery (unpublished data). The even slower dissociation kinetics of GFP-B23 from the nucleolus in comparison to the snoRNP components might reflect its function not only as a processing enzyme but also as a protein chaperone in the assembly of preribosomal subunits (Szebeni et al., 2003), which have longer residence time in nucleoli than the relatively short-lived pre-rRNA processing intermediates (Lazdins et al., 1997; Chen and Huang, 2001).

Kinetic independence of CBs and gems

The fact that coilin has one of the longest residence times of all CB components might suggest that it is a structural element. Consistent with this model, coilin is a multi-interactive protein that, apart from interacting with itself (Hebert and Matera, 2000; this paper), associates with SMN, SmB/B′ (Hebert et al., 2001), and Nopp140 (Isaac et al., 1998). However, loss of coilin in mice does not result in complete disappearance of CBs, but rather causes relocalization of various CB components into at least three distinct types of residual nuclear bodies, suggesting that coilin is not essential for the maintenance of nuclear compartments that contain many of the CB components (Tucker et al., 2001; Jady et al., 2003). Nevertheless, coilin does clearly play a critical role in recruitment of CB components to a combined CB/gem structure. Similarly, the SMN protein interacts with a multitude of partners including spliceosomal snRNPs and nucleolar snoRNPs, fibrillarin, GAR1, nucleolin, and B23 (Friesen and Dreyfuss, 2000; Jones et al., 2001; Pellizzoni et al., 2001; Lefebvre et al., 2002). However, in contrast to coilin, whose self-interaction domain targets it to CBs, SMN requires the presence of coilin for its recruitment into CBs (Hebert et al., 2001; Tucker et al., 2001). Despite the physical association and the direct interaction of coilin with SMN, CBs and gems are kinetically autonomous compartments because the dissociation kinetics of several respective components remain unchanged upon separation of the two structures. The basis for this kinetic autonomy may be the ability of SMN and coilin to maintain self-interactions within the separated nuclear bodies. These observations paint a picture in which two independent nuclear structures, the CB and gem, are spatially superimposed due to the dynamic interaction of their marker proteins.

One possible advantage of fusing the two structures into one spatially overlapping domain might be that the concentration of substrates (e.g., snRNPs) and enzymes (e.g., SMN complexes) increases the efficiency of RNA metabolism. Conceivably, SMN–snRNP complexes might localize to the CB after passage through nuclear pores; coilin could then dissociate this complex by competing for SMN's Sm-binding sites (Hebert et al., 2001). This would allow for modification of snRNAs by CB components such as the scaRNPs (Darzacq et al., 2002; Jady et al., 2003). However, such a pathway cannot be an obligate one, as coilin is not an essential protein. Another possibility is that gems represent a storage depot for excess nuclear SMN complexes, forming in response to the methylation status of coilin and/or Sm proteins. Clearly, uncovering the complex links between CBs and gems will require further investigation of the structural, functional, and dynamic relationships between these two nuclear subcompartments.

Materials and methods

Plasmid construction

Construction of GFP-coilin and GFP-coilin mutants (Hebert and Matera, 2000; Hebert et al., 2001), GFP-SmB and SmD1 (Sleeman and Lamond, 1999a), GFP-SART3 (Stanek et al., 2003), fibrillarin-GFP, protein B23-GFP (Dundr et al., 2000), GFP-GAR1 (Pogacic et al., 2000), GFP-U3-55k (Pluk et al., 1998), GFP-UBF1 (Dundr et al., 2002), GFP-SMN (Sleeman et al., 2001), and GFP-Tgs1 (Mouaikel et al., 2003) have been described as listed. GFP-Nopp140 (pTM95) was generated by cloning PCR-amplified GFP from pGreenLantern (CLONTECH Laboratories, Inc.) into pTM38 to which the COOH terminus of Nopp140 was added as described previously (Isaac et al., 1998). Gemin3-GFP was PCR amplified out of pcDNA-Gemin3 (Ou et al., 2001) before subcloning into pEGFP-N3 as a BglII–KpnI fragment. YFP-NHPX/15.5k (Leung and Lamond, 2002) was resubcloned into pEGFP-C1 as a BspE1–KpnI fragment. GFP-SMN was resubcloned into pECFP-C1 and pEYFP-C1 as a BspEI–EcoRI fragment. Untagged ΔRG coilin was subcloned into pCMV-sport6 vector.

Cell culture and transfection

HeLa wild-type, HeLa-PV, and MEFs were grown in DME (Invitrogen) supplemented with 10% FCS (Invitrogen), 1% glutamine, and penicillin and streptomycin at 37°C in 5% CO_2. The cells were electroporated with an electroporator (model ECM 830; BTX) using 5 μg plasmid DNA and 15 μg sheared salmon sperm carrier DNA in a 2-mm gap cuvette at 200 V, 1-ms pulse, 4 pulses, and 0.5-s intervals. After electroporation, the cells were plated in Lab-Tek® II chambers (Nalgene), and after ∼6 h the medium was changed to DME with 25 mM Hepes without phenol red (Invitrogen). In cotransfection experiments, the ratio of ΔRG-coilin to CFP-coilin (SMN) to YFP-SMN (coilin) was 3:1:1.

Photobleaching

iFRAP experiments were performed on a confocal microscope (LSM 510; Carl Zeiss MicroImaging, Inc.) with a 100×/1.3 N.A. Plan Apochromat oil objective and 3× zoom. GFP was excited with the 488-nm line of argon laser, and GFP emission was monitored above 505 nm as described previously (Dundr et al., 2002). Cells were maintained at 37°C with an Air Stream incubator (ASI 400; Nevtek). The whole nuclear area of transfected cells was bleached except for a small region of one CB using the 488-nm laser line at 100% laser power. Cells were monitored in 0.5-s intervals for 195 s. To minimize the effect of photobleaching due to imaging, images were collected at 0.1% laser intensity. For quantification, the loss of total fluorescent intensity in the unbleached region of interest was measured using software from Carl Zeiss MicroImaging, Inc. Background fluorescence was measured in a random field outside of the cells. For each time point, the relative loss of fluorescent intensity in the unbleached region of interest was calculated as: $I_{rel} = (I_{(t)} - BG)/(I_o - BG)*(T_{(t)} - BG)$, where I_o is the background-corrected average intensity of the region of interest during prebleach, and $T_{(t)}$ is the background-corrected total fluorescence intensity of a neighboring control cell. Typical measurement errors in all experiments were ∼15%. For statistical comparison of iFRAP data, *t* tests on t_{50} (defined as time after bleaching when 50% of the initial fluorescence signal was lost) were performed.

FRET

FRET experiments were performed on a confocal microscope (LSM 510; Carl Zeiss MicroImaging, Inc.) with a 100×/1.3 N.A. Plan Apochromat oil objective and 3× zoom. FRET was measured using the acceptor photobleaching method (Karpova et al., 2003). In the presence of FRET,

bleaching of the acceptor (YFP) results in a significant increase in fluorescence of the donor (CFP). A single CB was bleached for 500 ms in the YFP channel using the 514 argon laser line at 100% intensity. Before and after the bleach, CFP images were collected to assess changes in donor fluorescence. To minimize the effect of photobleaching due to imaging, images were collected at 0.1% laser intensity. To ensure that bleaching due to imaging was minimal, the level of bleaching in each experiment was monitored by collecting five CFP/YFP prebleach and postbleach image pairs. Each image was collected first in the CFP channel, and then in the YFP channel. The gain of the photomultiplier tubes was adjusted to obtain the best possible dynamic range. The FRET efficiency as a percentage of E_F was calculated as: $E_F = (I_{post} - I_{pre}) \times 100/I_{post}$, where I_{pre} is the prebleach CFP intensity in the last prebleach image, and I_{post} is the postbleach CFP intensity in the bleached region of the first post-bleach image. As a negative control, an unbleached CB in the same cell was measured, or FRET between monomeric CFP and YFP was measured in the nucleoplasm. As a positive control, a CFP-YFP fusion protein was used.

We thank Drs. E. Bertrand and R. Bordonne (IGMM-CNRS, Montpelier, France); A. Lamond, A. Leung, and M. Platani (University of Dundee, Dundee, UK); W. Filipowicz and V. Pogacic (Friedrich Miescher Institute for Biomedical Research, Basel, Switzerland); and G. Pruijn (University of Nijmegen, Nijmegen, Netherlands) for providing reagents. All imaging was performed at the National Cancer Institute Fluorescence Imaging Facility. T. Misteli is a fellow of the Keith R. Porter Endowment for Cell Biology.

This work was supported by National Institutes of Health grants GM53034 and NS41617 (to A.G. Matera).

Submitted: 21 November 2003
Accepted: 5 February 2004

References

Bell, M., S. Schreiner, A. Damianov, R. Reddy, and A. Bindereif. 2002. p110, a novel human U6 snRNP protein and U4/U6 snRNP recycling factor. *EMBO J.* 21:2724–2735.

Boisvert, F.M., M.J. Kruhlak, A.K. Box, M.J. Hendzel, and D.P. Bazett-Jones. 2001. The transcription coactivator CBP is a dynamic component of the promyelocytic leukemia nuclear body. *J. Cell Biol.* 152:1099–1106.

Boisvert, F.M., J. Cote, M.C. Boulanger, P. Cleroux, F. Bachand, C. Autexier, and S. Richard. 2002. Symmetrical dimethylarginine methylation is required for the localization of SMN in Cajal bodies and pre-mRNA splicing. *J. Cell Biol.* 159:957–969.

Boudonck, K., L. Dolan, and P.J. Shaw. 1999. The movement of coiled bodies visualized in living plant cells by the green fluorescent protein. *Mol. Biol. Cell.* 10:2297–2307.

Carmo-Fonseca, M. 2002. New clues to the function of the Cajal body. *EMBO Rep.* 3:726–727.

Carvalho, T., F. Almeida, A. Calapez, M. Lafarga, M.T. Berciano, and M. Carmo-Fonseca. 1999. The spinal muscular atrophy disease gene product, SMN: A link between snRNP biogenesis and the Cajal (coiled) body. *J. Cell Biol.* 147:715–728.

Chen, D., and S. Huang. 2001. Nucleolar components involved in ribosome biogenesis cycle between the nucleolus and nucleoplasm in interphase cells. *J. Cell Biol.* 153:169–176.

Darzacq, X., B.E. Jady, C. Verheggen, A.M. Kiss, E. Bertrand, and T. Kiss. 2002. Cajal body-specific small nuclear RNAs: a novel class of 2′-*O*-methylation and pseudouridylation guide RNAs. *EMBO J.* 21:2746–2756.

Dundr, M., T. Misteli, and M.O. Olson. 2000. The dynamics of postmitotic reassembly of the nucleolus. *J. Cell Biol.* 150:433–446.

Dundr, M., U. Hoffmann-Rohrer, Q. Hu, I. Grummt, L.I. Rothblum, R.D. Phair, and T. Misteli. 2002. A kinetic framework for a mammalian RNA polymerase in vivo. *Science.* 298:1623–1626.

Fischer, U., Q. Liu, and G. Dreyfuss. 1997. The SMN-SIP1 complex has an essential role in spliceosomal snRNP biogenesis. *Cell.* 90:1023–1029.

Friesen, W.J., and G. Dreyfuss. 2000. Specific sequences of the Sm and Sm-like (Lsm) proteins mediate their interaction with the spinal muscular atrophy disease gene product (SMN). *J. Biol. Chem.* 275:26370–26375.

Gall, J.G. 2000. Cajal bodies: the first 100 years. *Annu. Rev. Cell Dev. Biol.* 16: 273–300.

Handwerger, K.E., C. Murphy, and J.G. Gall. 2003. Steady-state dynamics of Cajal body components in the *Xenopus* germinal vesicle. *J. Cell Biol.* 160:495–504.

Hebert, M.D., and A.G. Matera. 2000. Self-association of coilin reveals a common theme in nuclear body localization. *Mol. Biol. Cell.* 11:4159–4171.

Hebert, M.D., P.W. Szymczyk, K.B. Shpargel, and A.G. Matera. 2001. Coilin forms the bridge between Cajal bodies and SMN, the spinal muscular atrophy protein. *Genes Dev.* 15:2720–2729.

Hebert, M.D., K.B. Shpargel, J.K. Ospina, K.E. Tucker, and A.G. Matera. 2002. Coilin methylation regulates nuclear body formation. *Dev. Cell.* 3:329–337.

Isaac, C., Y. Yang, and U.T. Meier. 1998. Nopp140 functions as a molecular link between the nucleolus and the coiled bodies. *J. Cell Biol.* 142:319–329.

Jady, B.E., X. Darzacq, K.E. Tucker, A.G. Matera, E. Bertrand, and T. Kiss. 2003. Modification of Sm small nuclear RNAs occurs in the nucleoplasmic Cajal body following import from the cytoplasm. *EMBO J.* 22:1878–1888.

Jones, K.W., K. Gorzynski, C.M. Hales, U. Fischer, F. Badbanchi, R.M. Terns, and M.P. Terns. 2001. Direct interaction of the spinal muscular atrophy disease protein SMN with the small nucleolar RNA-associated protein fibrillarin. *J. Biol. Chem.* 276:38645–38651.

Karpova, T.S., C.T. Baumann, L. He, X. Wu, A. Grammer, P. Lipsky, G.L. Hager, and J.G. McNally. 2003. Fluorescence resonance energy transfer from cyan to yellow fluorescent protein detected by acceptor photobleaching using confocal microscopy and a single laser. *J. Microsc.* 209:56–70.

Lazdins, I.B., M. Delannoy, and B. Sollner-Webb. 1997. Analysis of nucleolar transcription and processing domains and pre-rRNA movements by in situ hybridization. *Chromosoma.* 105:481–495.

Lefebvre, S., P. Burlet, L. Viollet, S. Bertrandy, C. Huber, C. Belser, and A. Munnich. 2002. A novel association of the SMN protein with two major nonribosomal nucleolar proteins and its implication in spinal muscular atrophy. *Hum. Mol. Genet.* 11:1017–1027.

Leung, A.K., and A.I. Lamond. 2002. In vivo analysis of NHPX reveals a novel nucleolar localization pathway involving a transient accumulation in splicing speckles. *J. Cell Biol.* 157:615–629.

Lorson, C.L., J. Strasswimmer, J.M. Yao, J.D. Baleja, E. Hahnen, B. Wirth, T. Le, A.H. Burghes, and E.J. Androphy. 1998. SMN oligomerization defect correlates with spinal muscular atrophy severity. *Nat. Genet.* 19:63–66.

Liu, Q., and G. Dreyfuss. 1996. A novel nuclear structure containing the survival of motor neurons protein. *EMBO J.* 15:3555–3565.

Liu, J., M.D. Hebert, Y. Ye, D.J. Templeton, H. Kung, and A.G. Matera. 2000. Cell cycle-dependent localization of the CDK2-cyclin E complex in Cajal (coiled) bodies. *J. Cell. Sci.* 113:1543–1552.

Matera, A.G. 1999. Nuclear bodies: multifaceted subdomains of the interchromatin space. *Trends Cell Biol.* 9:302–309.

Matera, A.G., and M.R. Frey. 1998. Coiled bodies and gems: Janus or gemini? *Am. J. Hum. Genet.* 63:317–321.

Meister, G., C. Eggert, and U. Fischer. 2002. SMN-mediated assembly of RNPs: a complex story. *Trends Cell Biol.* 12:472–478.

Mouaikel, J., U. Narayanan, C. Verheggen, A.G. Matera, E. Bertrand, J. Tazi, and R. Bordonne. 2003. Interaction between the small-nuclear-RNA cap hypermethylase and the spinal muscular atrophy protein, survival of motor neuron. *EMBO Rep.* 4:616–622.

Narayanan, U., J.K. Ospina, M.R. Frey, M.D. Hebert, and A.G. Matera. 2002. SMN, the spinal muscular atrophy protein, forms a pre-import snRNP complex with snurportin1 and importin beta. *Hum. Mol. Genet.* 11:1785–1795.

Ochs, R.L., T.W.J. Stein, and E.M. Tan. 1994. Coiled bodies in the nucleolus of breast cancer cells. *J. Cell Sci.* 107:385–399.

Ogg, S.C., and A.I. Lamond. 2002. Cajal bodies and coilin–moving towards function. *J. Cell Biol.* 159:17–21.

Ou, Q., J.F. Mouillet, X. Yan, C. Dorn, P.A. Crawford, and Y. Sadovsky. 2001. The DEAD box protein DP103 is a regulator of steroidogenic factor-1. *Mol. Endocrinol.* 15:69–79.

Paushkin, S., A.K. Gubitz, S. Massenet, and G. Dreyfuss. 2002. The SMN complex, an assemblyosome of ribonucleoproteins. *Curr. Opin. Cell Biol.* 14: 305–312.

Pellizzoni, L., J. Baccon, B. Charroux, and G. Dreyfuss. 2001. The survival of motor neurons (SMN) protein interacts with the snoRNP proteins fibrillarin and GAR1. *Curr. Biol.* 11:1079–1088.

Phair, R.D., and T. Misteli. 2000. High mobility of proteins in the mammalian cell nucleus. *Nature.* 404:604–609.

Phair, R.D., S.A. Gorski, and T. Misteli. 2004. Measurement of dynamic protein binding to chromatin in vivo, using photobleaching microscopy. *Methods Enzymol.* 375:393–414.

Platani, M., I. Goldberg, J.R. Swedlow, and A.I. Lamond. 2000. In vivo analysis of Cajal body movement, separation, and joining in live human cells. *J. Cell Biol.* 151:1561–1574.

Platani, M., I. Goldberg, A.I. Lamond, and J.R. Swedlow. 2002. Cajal body dynamics and association with chromatin are ATP-dependent. *Nat. Cell Biol.* 4:502–508.

Pluk, H., J. Soffner, R. Luhrmann, and W. J. van Venrooij. 1998. cDNA cloning and characterization of the human U3 small nucleolar ribonucleoprotein complex-associated 55-kilodalton protein. *Mol. Cell. Biol.* 18:488–498.

Pogacic, V., F. Dragon, and W. Filipowicz. 2000. Human H/ACA small nucleolar RNPs and telomerase share evolutionarily conserved proteins NHP2 and NOP10. *Mol. Cell. Biol.* 20:9028–9040.

Raska, I., L.E. Andrade, R.L. Ochs, E.K. Chan, C.M. Chang, G. Roos, and E.M. Tan. 1991. Immunological and ultrastructural studies of the nuclear coiled body with autoimmune antibodies. *Exp. Cell Res.* 195:27–37.

Shpargel, K.B., J.K. Ospina, K.E. Tucker, A.G. Matera, and M.D. Hebert. 2003. Control of Cajal body number is mediated by the coilin C-terminus. *J. Cell Sci.* 116:303–312.

Sleeman, J.E., and A.I. Lamond. 1999a. Newly assembled snRNPs associate with coiled bodies before speckles, suggesting a nuclear snRNP maturation pathway. *Curr. Biol.* 9:1065–1074.

Sleeman, J.E., and A.I. Lamond. 1999b. Nuclear organization of pre-mRNA splicing factors. *Curr. Opin. Cell Biol.* 11:372–377.

Sleeman, J., C.E. Lyon, M. Platani, J.P. Kreivi, and A.I. Lamond. 1998. Dynamic interactions between splicing snRNPs, coiled bodies and nucleoli revealed using snRNP protein fusions to the green fluorescent protein. *Exp. Cell Res.* 243:290–304.

Sleeman, J.E., P. Ajuh, and A.I. Lamond. 2001. snRNP protein expression enhances the formation of Cajal bodies containing p80-coilin and SMN. *J. Cell Sci.* 114:4407–4419.

Sleeman, J.E., L. Trinkle-Mulcahy, A.R. Prescott, S.C. Ogg, and A.I. Lamond. 2003. Cajal body proteins SMN and Coilin show differential dynamic behaviour in vivo. *J. Cell Sci.* 116:2039–2050.

Snaar, S., K. Wiesmeijer, A.G. Jochemsen, H.J. Tanke, and R.W. Dirks. 2000. Mutational analysis of fibrillarin and its mobility in living human cells. *J. Cell Biol.* 151:653–662.

Stanek, D., S.D. Rader, M. Klingauf, and K.M. Neugebauer. 2003. Targeting of U4/U6 small nuclear RNP assembly factor SART3/p110 to Cajal bodies. *J. Cell Biol.* 160:505–516.

Szebeni, A., K. Hingorani, S. Negi, and M.O. Olson. 2003. Role of protein kinase CK2 phosphorylation in the molecular chaperone activity of nucleolar protein b23. *J. Biol. Chem.* 278:9107–9115.

Tucker, K.E., M.T. Berciano, E.Y. Jacobs, D.F. LePage, K.B. Shpargel, J.J. Rossire, E.K. Chan, M. Lafarga, R.A. Conlon, and A.G. Matera. 2001. Residual Cajal bodies in coilin knockout mice fail to recruit Sm snRNPs and SMN, the spinal muscular atrophy gene product. *J. Cell Biol.* 154:293–307.

Verheggen, C., D.L. Lafontaine, D. Samarsky, J. Mouaikel, J.M. Blanchard, R. Bordonne, and E. Bertrand. 2002. Mammalian and yeast U3 snoRNPs are matured in specific and related nuclear compartments. *EMBO J.* 21:2736–2745.

Wei, Y., J. Jin, and J.W. Harper. 2003. The cyclin E/Cdk2 substrate and Cajal body component p220(NPAT) activates histone transcription through a novel LisH-like domain. *Mol. Cell. Biol.* 23:3669–3680.

Young, P.J., T.T. Le, N. thi Man, A.H. Burghes, and G.E. Morris. 2000. The relationship between SMN, the spinal muscular atrophy protein, and nuclear coiled bodies in differentiated tissues and cultured cells. *Exp. Cell Res.* 256: 365–374.

Young, P.J., T.T. Le, M. Dunckley, T.M. Nguyen, A.H. Burghes, and G.E. Morris. 2001. Nuclear gems and Cajal (coiled) bodies in fetal tissues: nucleolar distribution of the spinal muscular atrophy protein, SMN. *Exp. Cell Res.* 265:252–261.

Zhu, Y., R.L. Tomlinson, A.A. Lukowiak, R.M. Terns, and M.P. Terns. 2004. Telomerase RNA accumulates in Cajal bodies in human cancer cells. *Mol. Biol. Cell.* 15:81–90.